Journal of Biomedical Optics

BiomedicalOptics.SPIEDigitalLibrary.org

Two-stage multi-Gaussian fitting of conduit artery photoplethysmography waveform during induced unilateral hemodynamic events

Andris Grabovskis
Zbignevs Marcinkevics
Uldis Rubins
Juris Imants Aivars

SPIE.

Two-stage multi-Gaussian fitting of conduit artery photoplethysmography waveform during induced unilateral hemodynamic events

Andris Grabovskis,[a,*] Zbignevs Marcinkevics,[b] Uldis Rubins,[a] and Juris Imants Aivars[b]
[a]University of Latvia, Institute of Atomic Physics and Spectroscopy, Raina Boulevard 19, Riga LV-1586, Latvia
[b]University of Latvia, Faculty of Biology, Department of Human and Animal Physiology, Raina Boulevard 19, Riga LV-1586, Latvia

Abstract. Photoplethysmography (PPG) is an optical technique with high diagnostic potential, yet clinical applications remain underdeveloped. Standardization of signal recording and quantification of waveform are essential prerequisites for broader clinical use. The aim of this study was to utilize a two-stage multi-Gaussian fitting technique in order to examine the parameters of conduit artery PPG waveform recorded during increasing the unilateral regional vascular resistance (RVR). This study was conducted on 14 young and healthy volunteers; various external compressions (ECs) were performed by inflating a tight cuff at 0, 40, 80, and 200 mmHg, while registering femoral PPG (wavelength 880 nm), diameter, blood flow linear velocity (vascular ultrasound), and the arterial pressure (Finapres) during the states of the baseline, partial, and total arterial occlusion, and resultant reactive hyperemia. An increase of the EC elevated the arterial stiffness (AS) and the unilateral distal RVR, and caused a shift of the fitted multi-Gaussian parameters: a decreased delay between reflected and traverse wave components and an increased ratio of their amplitudes. It was concluded that two-stage multi-Gaussian waveform quantification demonstrates an approach potentially extending the use of arterial site PPG in the assessment of diagnostically useful markers e.g., the RVR and the AS. [DOI: 10.1117/1.JBO.20.3.035001]

Keywords: arterial photoplethysmography; waveform decomposition; Gaussian function; external compression.

Paper 140727LR received Nov. 4, 2014; accepted for publication Feb. 19, 2015; published online Mar. 9, 2015; corrected Mar. 23, 2015.

1 Introduction

Photoplethysmography (PPG) is a well-recognized optical technique for noninvasive arterial pulsation detection. It was originated in the beginning of the 20th century and is still a burgeoning field of biomedical engineering currently presented in numerous R&D and application studies. However, despite its high diagnostic potential, PPG has yielded clinical applications only in a few specific areas such as the assessment of blood oxygenation known as the pulse oximetry or, in minor cases, as the technique for vascular tone/age estimation from the pulse waveform. Such PPG utilization is being reported in several prominent reviews.[1,2] In conventional applications, PPG is registered from diffuse vascular beds e.g., distal phalanxes or the earlobe, comprising small caliber arterioles, venules, and capillaries.[1,2–4] There are only a few reports describing PPG signal recording from superficial conduit arterial sites[5–7] that could potentially gain more specific information of the hemodynamics e.g., the arterial stiffness (AS).[8] The major reasons for the limited use of PPG in the routine clinical assessment of the vascular state are the waveform quantification and measurement procedure standardization issues. Among several studies on such PPG waveform quantification, there is a lack of reports on single period PPG (SPPPG) waveform dynamics during hemodynamic maneuvers, such as altering the regional vascular resistance (RVR), increasing the blood flow shear, and others, particularly on the PPG signal obtained from superficial conduit artery sites. A literature review reveals that our study is one of the few addressing this issue. A similar procedure utilizing ultrasound (US) to examine the pulsations of femoral artery distension and blood flow velocity during manipulations of RVR has been reported by Heffernan et al.[9] It is generally accepted that the rising distally performed external compression (EC) quantitatively mimics an increase of unilateral RVR and such provocation of hemodynamic response is utilized in physiologic research.[9,10] Peripheral vascular resistance is recognized as an important indicator of different infectious syndromes, diseases, and general vascular age. Therefore, understanding the RVR relationship to SPPPG waveform and its potential quantification has a crucial role in the extension of clinical applications of PPG[11] and brings motivation to this preliminary study.

Generally, the accepted approach in the assessment of hemodynamic parameters from the single arterial pulse waveform is a segregation of its feature points (FPs). Prominent studies have already described the extraction of FP from SPPPG waveform[4,12] or its derivatives,[13] or by fitting various types, combinations, and numbers of analytic functions.[14,15] In cases of a damped, monotonically decreasing diastolic part, existing models often reveal limited operating range and inconsistent calculation of FP.[16] Meanwhile, the similarity of a single hemodynamic wave component, i.e., the left ventricle ejection volume profile and the Gaussian function profile, has previously been reported and utilized[17,18] and can also be visually noticed.[19]

*Address all correspondence to: Andris Grabovskis, E-mail: andris.grabovskis@gmail.com

1083-3668/2015/$25.00 © 2015 SPIE

Recent studies employ a multi-Gaussian model for fitting the peripheral pulse waveform[20–22] guided by the criterion of minimal root-mean-square error (RMSE). An approximation of the SPPPG waveform with four Gaussian functions has also been demonstrated by our group highlighting its advantages over the derivative analysis.[17] However, such previous studies were predominantly focused on fitting accuracy rather than the relevance of actual physiological pulse waves to Gaussian model components, while only a single case mentions their possible pertinence.[18] Apparently, based only on the minimal RMSE criterion, the multi-Gaussian model cannot be used for such an explanation, as the variability of pulse waveform contour causes chaotic dissipation of the fitted components.

Our results indirectly indicate that in designing a reliable Gaussian-based hemodynamic model, boundary conditions for the pulse component positioning and scaling are required.

The present study explores the potential of conduit artery PPG in evaluating the hemodynamic events. The aim of this study was to utilize a two-stage multi-Gaussian fitting technique in order to examine the parameters of conduit artery SPPPG waveform recorded during increasing the unilateral RVR. We hypothesized that by altering the leg's RVR and AS via the tight EC test, femoral pulse waveform transforms, and this resonates in a component shift of SPPPG waveform and fitted multi-Gaussian model.

2 Methods

This study was approved by the Ethics Committee of the University of Latvia, Institute of Experimental and Clinical Medicine, and, with their informed consent, it was performed by enrolling 14 subjects (6 male, 8 female, 25 ± 5 years old). To ensure adequate vascular response, the subjects were asked to refrain from caffeine drinks and active workload for at least 8 h prior to the experiment. In order to improve PPG signal quality, isolate uncontrolled conditions and simplify the palpation of the arterial site for correct PPG/US probe location, enrolled subjects were ectomorph body type (body mass index <20) nonsmoking and normotensive. During the procedure, subjects were held in supine position in a quiet, warm (23°C to 25°C) and comfortable room.

The study protocol included data acquisition of different modalities at the rest, during and after the provocation test; signal processing and hemodynamic parameter calculation, and statistical analysis, Fig. 1.

To provoke regional hemodynamic responses in the femoral artery and distal arterial bed, the study protocol comprised five consecutive measurement states (MS) induced by various tight ECs with CC17 Contoured Thigh Cuff, E20 Inflator and AG101 air supply (D. E. Hokanson, Inc., USA): the baseline MS1 at the rest conditions with 0 mmHg external cuff pressure, the states of partial arterial occlusion MS2 and MS3 (40 and 80 mmHg cuff pressure, each for 15 s), total arterial occlusion MS4 (200 mmHg cuff pressure for 300 s), and the resultant reactive hyperemia (RH) MS5 monitored for the first 30 s, similar to that described by Heffernan et al.[9]

During the aforementioned MS, three different signal modalities were simultaneously recorded: PPG ($\lambda = 880$ nm) from the femoral artery site close to the inguinal ligament utilizing the optimal sensor contact force approach;[23] simultaneous Doppler and B mode US 12L-RS, LOGIQe (GE Medical Systems, USA), positioned approximately 1 cm distally to the PPG probe, recording both the longitudinal section of the artery (diameter d) and the profile of blood flow time averaged mean (TAM) velocity v, Fig. 2; and systolic, diastolic and mean blood pressure values acquired from Finometer Model2 in a beat-per-beat manner and calibrated to brachial arterial pressure (Finapres Medical Systems, The Netherlands).

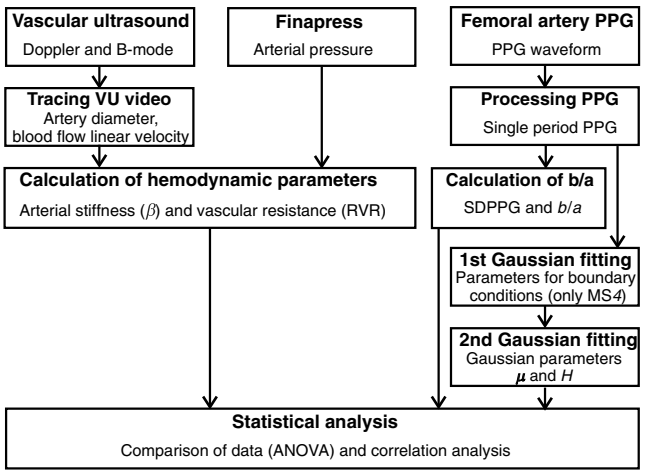

Fig. 1 Flowchart of the performed protocol. β and b/a – local arterial stiffness indices; RVR – regional vascular resistance; SDPPG – second derivative of PPG waveform; MS4 – measurement state of total arterial occlusion; H – Gaussian peak amplitude, μ – Gaussian peak time delay in the waveform.

Data analysis was performed offline in three major steps. First, artifacts of US data were excluded and both the blood flow and diameter traces were determined from the US videos by a custom made MATLAB® US image recognition software.[24] Then, PPG processing was performed by stating the valid range of SPPPG waveform length equal to the median absolute deviation $T\mathrm{mad}_{\mathrm{state}}$ in each of the MS from the corresponding dataset; hence, valid and ectopic waveforms were determined and separated by the criterion:

$$|T_{\mathrm{state}} - T_{\mathrm{ins}}| < T\mathrm{mad}_{\mathrm{state}}, \tag{1}$$

where T_{state} is the median pulse duration within each MS and T_{ins} is the duration of the inspected pulse within the same MS. Then, the returned, i.e., valid SPPPG waveforms were resampled at 1 kHz to 1 s length with a spline interpolation technique and normalized to 1 a. u.

A comparison of amplitudes of valid waveforms from all MS was performed in every sample $j|_0^{1000}$. Inspected SPPPG waveform amplitude a_j was compared to the mean amplitude within each MS A_j and the waveform was excluded if the squared difference exceeded the RMSE at any of the waveform samples:

$$(A_j - a_j)^2 > \mathrm{ARMSE}_j, \tag{2}$$

where ARMSE_j is an RMSE of the same inspected SPPPG waveform at the sample j, thereby picking SPPPG waveforms that characterize each state of the performed measurement. Subsequently, one representative SPPPG waveform per MS was calculated as the median contour of each MS dataset. In the second step, all processed data were merged in a single data array in beat-per-beat manner (synchronized time series). Third, the parameters describing the induced hemodynamic response were calculated and stored in a .mat file for statistical analysis. During each MS, the RVR was graded as

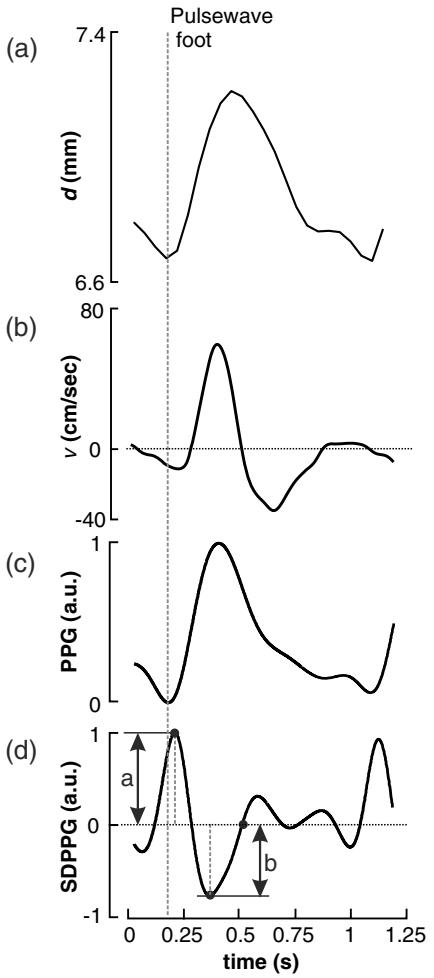

Fig. 2 Typical example of femoral artery pulsation waveforms during the rest conditions (MS1): (a) diameter *d*, (b) blood flow linear TAM velocity *v*, (c) both acquired simultaneously with US; (d) single period arterial PPG and its second derivative SDPPG. SDPPG inflection points *a* and *b* are used for the assessment of the local arterial stiffness.

$$\mathrm{RVR}_{\mathrm{femoral}} = \mathrm{MAP}/Q, \tag{3}$$

where Q is the total femoral blood flow and MAP is the mean arterial pressure,[25] while the changes of local AS were estimated with the referent index β:[26]

$$\beta = \frac{\ln(p_s/p_d)}{(d_s - d_d)/d_d}, \tag{4}$$

where p_s, p_d and d_s, d_d are the values of blood pressure and lumen diameter at systole and diastole, respectively. The pulse wave reflection index[9] was calculated as the ratio of retrograde to anterograde TAM velocity $v_{\mathrm{ret}}/v_{\mathrm{ant}}$ derived from the US signal, while an already approved indicator of local AS - SPPPG second derivative (SDPPG) index b/a[13] was calculated from the PPG signal in all MS.

Meanwhile, in order to manage SPPPG decomposition and waveform parameterization, preprocessed representative waveforms of each subject (one per every MS) were approximated with multiple (2 or 4) one-dimensional Gaussian functions in two fitting stages. In the first stage, the MS4 waveform was fitted with 2 Gaussians: $g_n(t, H, \mu, \sigma)$ where $n = 2$ is the number of Gaussian functions fitted in the SPPPG wave, H is the Gaussian peak amplitude, μ is the peak time delay in the waveform, and σ is the wave width, by solving the system of equations for the multi-Gaussian model $f_G(t)$, Fig. 3:

$$f_G(t) = \sum_n H_n e^{-\frac{(t-\mu_n)^2}{2\sigma_n^2}}. \tag{5}$$

Model parameters were estimated by the weighted least-squares method, minimizing the weighted sum of squared residuals:[27]

$$\sum_{j=1}^{1000} (\mathrm{SPPPG}_j - f_{Gj})^2 \to 0. \tag{6}$$

During the fitting the accuracy was estimated and demonstrated as residual graphs, Fig. 3.

The values of Gaussian parameters H, μ, and σ at this stage were set to boundary condition variables, and the second fitting stage was performed on all but MS4 waveforms by repeating the same approach (5–6) with $n = 4$ in compliance with the boundary conditions to determine Gaussian localization in the SPPPG signal in order to associate them to physiologic pulse wave components. Based on the assumptions of femoral site pulse wave component morphology, mentioned in Sec. 4, to the best of our knowledge, we hereby stated such boundary conditions for the first time. The time difference between both Gaussians $g1$ and $g3$ $\mu_3 - \mu_1$ was defined constant in all MS. Meanwhile, during all but MS4, the time difference between Gaussian pairs $g1 \sim g2$ and $g3 \sim g4$ was equal within the same MS: $\mu_2 - \mu_1 = \mu_4 - \mu_3$. During MS4, it was assumed $\mu_2 - \mu_1 = \mu_4 - \mu_3 = 0$ i.e., the SPPPG waveform during total arterial occlusion was fitted with two Gaussians. During the second fitting stage, four Gaussians were locked in a pair of double-Gaussians $g1 + g3$ and $g2 + g4$ allowing for varying only the time delay $\mu_2 - \mu_1$ and the Gaussian amplitudes that were allowed varying as $H_1 > H_2 > H_4$ and $H_1 > H_3 > H_4$ within the same MS.

Following this procedure, the variables derived from the SDPPG and the multi-Gaussian model were used to estimate the effect of EC on the SPPPG pulse contour and also to assess and validate the changes of leg local and regional AS. First, the values of both local AS indices - b/a and β were compared in all MS. Meanwhile during all but MS4 the regional AS of leg's arterial bed was indicated with the pulse transit time (PTT) $\mu_2 - \mu_1$ of the traverse pulse wave components i.e., $g1$ and $g3$ reaching the endpoint of leg arterial tree and traveling backwards to the PPG probe as $g2$ and $g4$ respectively. Leg peripheral wave reflection properties were described as a ratio of the reflected wave component to its systolic traverse origin, i.e., H_2/H_1 and intended to compare to the $v_{\mathrm{ret}}/v_{\mathrm{ant}}$.

The statistical analysis of the aforementioned parameters was performed on SigmaPlot by comparing the sets of data series by one way ANOVA. The relation of parameters was determined by Pearson correlation.

3 Results

Data from the US indicated the effect of EC on the RVR, expressed as mmHg/ml/ min. RVR obtained at the femoral site varied within the subject group from 0.57 ± 0.11; 0.97 ± 0.18, and 1.11 ± 0.20 at the MS1, MS2, and MS3, respectively, and

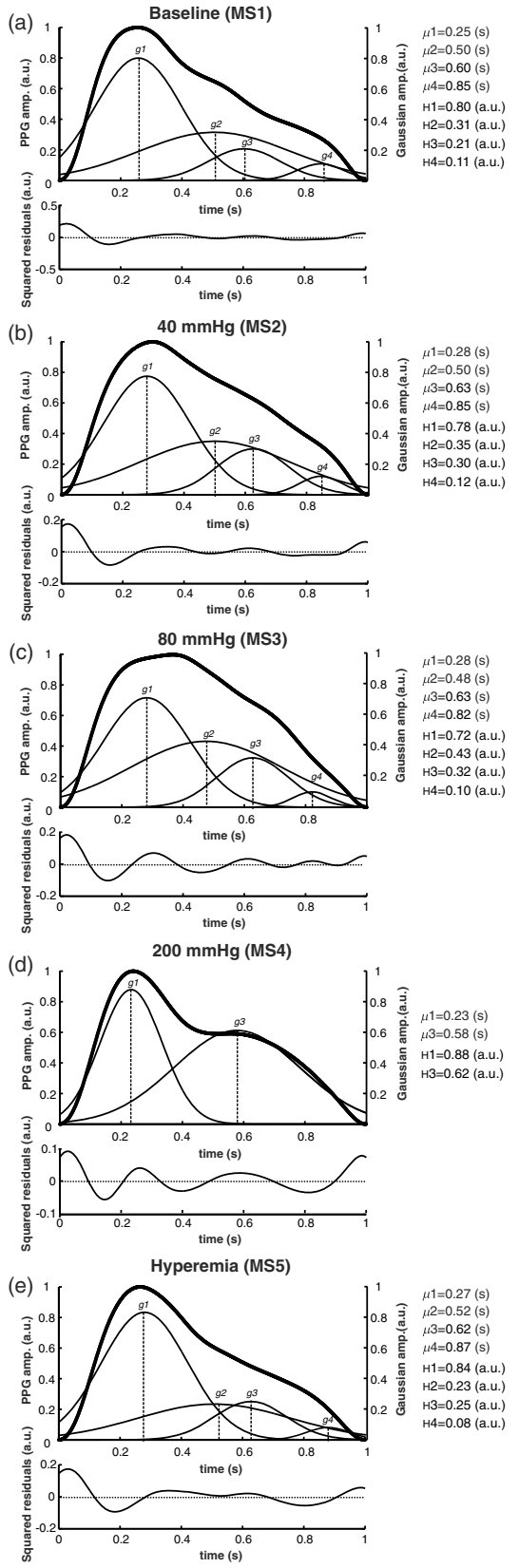

Fig. 3 Representative example (one subject data) of femoral SPPPG waveforms and the fitted Gaussians (upper plots) and the squared residuals (bottom plots) at the measurement states MS1 to MS5, influenced by the distal tight compression: (a) the baseline, (b) and (c) partial arterial occlusions 40 and 80 mmHg of cuff pressure, (d) total arterial occlusion at 200 mmHg, and (e) hyperemia; Gaussian components $g1$ to $g4$, and their respective peak amplitude H and time delay μ tabulated beside.

reached 3.36 ± 0.34 during MS4. In MS5, the release of the cuff caused RH and RVR to drop to 0.10 ± 0.02. Here and hereafter values are expressed as mean $\pm$ standard error of the mean (SEM.) Such RVR alterations were accompanied by significant changes of the v_{ret}/v_{ant}: consequently it increased from 0.392 ± 0.051 during MS1, to 0.747 ± 0.032 at MS2, and 0.820 ± 0.056 at MS3. The v_{ret}/v_{ant} during MS4 was 0.606 ± 0.056, however, due to the artificial pulse wave reflection conditions and the

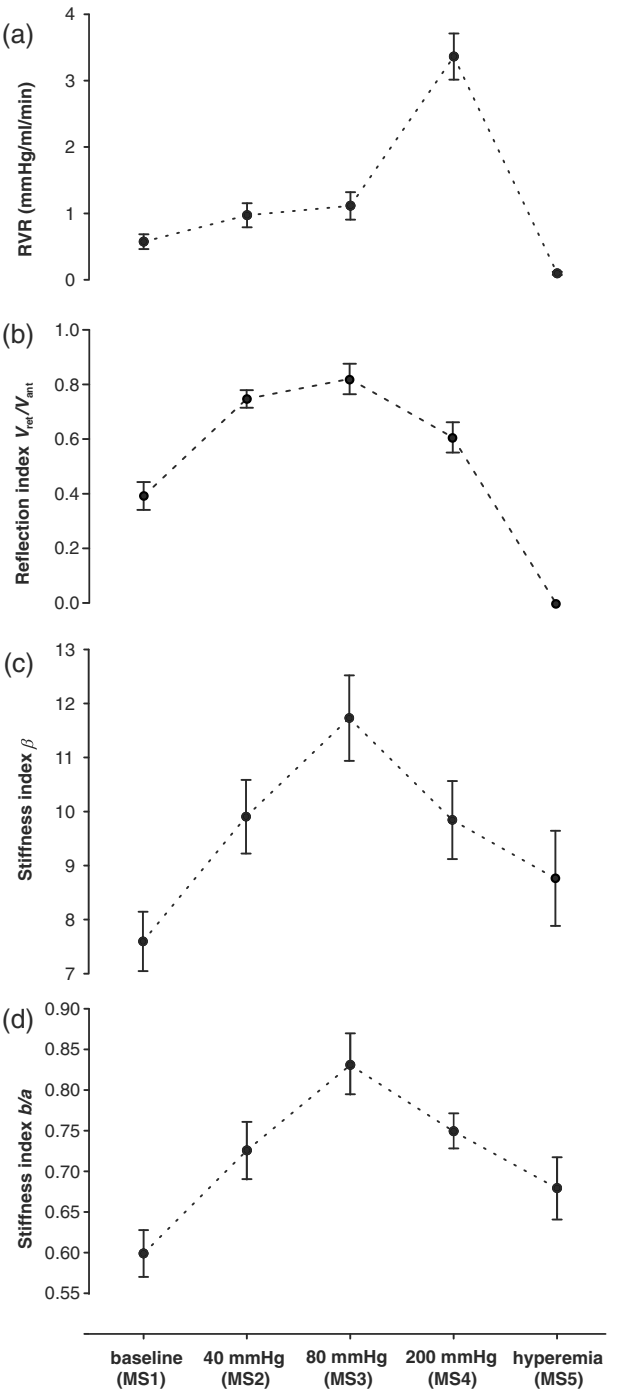

Fig. 4 Femoral artery regional hemodynamic parameters within the subject group at different external cuff pressures, data points, and error bars represent the mean $\pm$ standard error of the mean (SEM): (a) regional vascular resistance RVR; (b) pulse wave reflection index v_{ret}/v_{ant}; (c) local arterial stiffness indices β, and (d) b/a obtained by US and PPG techniques, respectively.

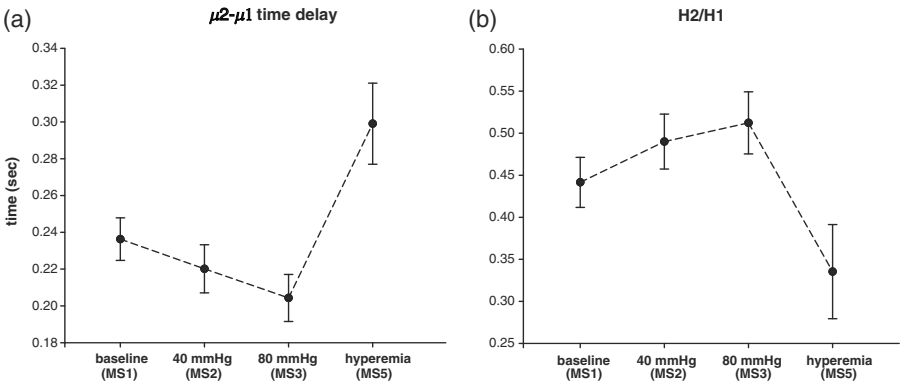

Fig. 5 The time delay between the traverse $g1$ and reflected $g2$ waves: (a) components $\mu_2 - \mu_1$ decreases while their amplitude ratio, (b) H_2/H_1 increases during all but MS4 measurement state, indicating an augmentation of distal vascular tone and resistance during raising external compression, data points, and error bars represent the mean $\pm$ SEM.

diminished blood flow velocity, it should be cautiously interpreted. During the RH in MS5 there is an absence of the retrograde blood flow component, thus the v_{ret}/v_{ant} was 0.

Meanwhile, a high correlation between the b/a and β at all the performed MS ($r = 0.97$, $p < 0.001$) was observed, proving the conformity of both local AS measures derived from PPG and US techniques, Fig. 4.

Four-Gaussian model parameters exhibited the changes of the SPPPG waveform, depending upon the EC: $\mu_2 - \mu_1$ declined from 0.236 ± 0.011 during the MS1 to 0.220 ± 0.013 and 0.204 ± 0.012 during partial arterial occlusions MS2 and MS3; while, on the contrary, H_2/H_1 increased from 0.442 ± 0.030 to 0.490 ± 0.033 and 0.51 ± 0.037 during the same MS of rising EC. Then, both parameters demonstrated a mutually inverse response to the RH: $\mu_2 - \mu_1$ increased to 0.299 ± 0.022 while H_2/H_1 dropped to 0.335 ± 0.056, Fig. 5.

4 Discussion

Our computed hemodynamic parameters during the performed maneuvers showed a similar systemic response to the EC as reported by Heffernan et al.[9] In addition to their performance, we calculated the numeric value of the leg's RVR in each MS and noticed only minor RVR changes between the baseline (MS1) and partial occlusions (MS2 and MS3). In those same MS with raising EC, both local AS indices b/a and β obtained by PPG and US showed an augmentation as expected. However, RVR demonstrated significant alterations during the arterial occlusion (MS4) and RH (MS5). The obtained values of local AS indices b/a and β showed good conformity with the previous results.[9,28]

Regarding the wave reflective properties of leg vasculature, rising RVR causes an augmentation of the reflected wave component expressed through the H_2/H_1. We refer it to as the v_{ret}/v_{ant}, while Heffernan et al describe this effect through the negative area of a pulse pressure wave. We share the view of the risen EC effect on the wave reflection through the diminished capacitance, i.e., reservoir function, thus constricting blood flow discharge into the periphery.[9]

As to the PPG waveform parametrization, the novelty of this study mostly relies on the MS4 conditions providing the necessary PPG waveform for the initial stage of fitting the Gaussians. We thereby assume that the femoral SPPPG pulse wave during MS of the total distal arterial occlusion in a sense represents an aortic pulse, as the peripheral vascular compliance is uncoupled by the inflated pressure cuff and serves as an artificial high vascular resistance reflection site. Such femoral pulse wave consists of two traverse waves: an ejection wave in the systole $g1$ and its re-reflection $g3$ in the diastole emerging between the bifurcation and aortic valve, Fig. 3(d). The pulse wave in this MS condition is not damped by the peripheral blood flow discharge and represents the combination of properties of heart function (pulse duration) and aortic elasticity (aortic PTT). We considered the $\mu_3 - \mu_1$ to correspond to the double bifurcation-to-aortic valve PTT of relevant subjects, which corresponds to the published data.[29] During the MS4, the PTT in the path probe-cuff-probe is close to zero due to their close proximity, while the pulse waves from all other MS contain reflected components $g2$ and $g4$ traveling from the endpoint of the leg periphery with a noticeably longer PTT. Indeed, a half of $\mu_2 - \mu_1$ as well as $\mu_4 - \mu_3$ during all but MS4 waveforms is also close to the PTT values of the pulse wave traveling from femoral to tibial sites at rest conditions.[5,30] If $\mu_2 - \mu_1$ is associated with the regional leg AS, it follows that the arterial tone augments during partial ischemia. Such an increase of AS in the distal vascular bed during EC trials has previously been reported.[31] $\mu_2 - \mu_1$ thereby consists of PTT components from the sites both distal and proximal to the cuff, and describes the total response of leg vasculature to the EC. Based on these assumptions, each fitted Gaussian is associated to the corresponding pulse wave component, and, by locking them in a pair of double-Gaussians – traverse double-wave $g1 + g3$ and reflected double-wave $g2 + g4$, the morphology of femoral artery pulsation waveform is described. Because of the locking, the fitting accuracy is sometimes sacrificed while the fitting accuracy obtained by a single double-Gaussian during MS4 meets previously obtained residual values.[17]

5 Conclusion

The femoral PPG waveform parameters derived from two-stage multi-Gaussian fitting quantitatively characterize their alterations upon the rising distal external compression causing a wide range hemodynamic events. The attempt of associating the Gaussians with pulse wave components demonstrates a new approach potentially extending the use of the arterial site PPG technique in the assessment of diagnostically useful clinical markers such as the peripheral vascular resistance and the arterial stiffness.

Acknowledgments

Financial support from European Union Social and R&D Funds, project nos. 2009/0138/1DP/1.1.2.1.2/09/IPIA/VIAA/004 and 2011/0045/2DP/2.1.1.3.1/11/IPIA/VIAA/001, is highly appreciated.

References

1. J. Allen, "Photoplethysmography and its application in clinical physiological measurement," *Physiol. Meas.* **28**(3), 1–39 (2007).
2. M. Nitzan, A. Romem, and R. Koppel, "Pulse oximetry: fundamentals and technology update," *Med. Devices* **8**(7), 231–239 (2014).
3. G. Tanaka et al., "A novel photoplethysmography technique to derive normalized arterial stiffness as a blood pressure independent measure in the finger vascular bed," *Physiol. Meas.* **32**, 1869–1883 (2011).
4. S. Alty et al., "Predicting arterial stiffness from the digital volume pulse waveform," *IEEE Trans. Biomed. Eng.* **54**(12), 2268–2275 (2007).
5. J. Weinman and D. Sapoznikov, "Equipment for continuous measurements of pulse wave velocities," *Med. Biol. Eng.* **9**, 125–138 (1971).
6. M. Eliakim, D. Sapoznikov, and J. Weinman, "Assessment of the atrial contribution to cardiac performance by a noninvasive photoplethysmographic technique," *Cardiology* **58**, 7–13 (1973).
7. S. Loukogeorgakis et al., "Validation of a device to measure arterial pulse wave velocity by a photoplethysmographic method," *Physiol. Meas.* **23**(3), 581–596 (2002).
8. A. Grabovskis et al., "Usability of photoplethysmography method in estimation of conduit artery stiffness," *Proc. SPIE* **8090**, 80900X (2011).
9. K. S. Heffernan et al., "Manipulation of arterial stiffness, wave reflections, and retrograde shear rate in the femoral artery using lower limb external compression," *Physiol. Rep.* **1**(2), e00022 (2013).
10. D. H. Thijssen et al., "Retrograde flow and shear rate acutely impair endothelial function in humans," *Hypertension* **53**, 986–992 (2009).
11. A. A. Awad et al., "The relationship between the photoplethysmographic waveform and systemic vascular resistance," *J. Clin. Monit. Comput.* **21**, 365–372 (2007).
12. S.C. Millaseau, M. J. Ritter, and K. Takazawa, "Contour analysis of the photoplethysmographic pulse measured at the finger," *J. Hypertens.* **24**(8), 1449–1456 (2006).
13. K. Takazawa et al., "Assessment of vasoactive agents and vascular aging by the second derivative of photoplethysmogram waveform," *Hypertension* **32**, 365–370 (1998).
14. M. C. Baruch et al., "Pulse decomposition analysis of the digital arterial pulse during hemorrhage simulation," *Nonlinear Biomed. Phys.* **5**(1), 1–15 (2011).
15. M. Huotari et al., "Photoplethysmography and its detailed pulse waveform analysis for arterial stiffness," *J. Struct. Mech.* **44**(4), 345–362 (2011).
16. L. A. Bortolotto et al., "Assessment of vascular aging and atherosclerosis in hypertensive subjects: second derivative of photoplethysmogram versus pulse wave velocity," *Am. J. Hypertens.* **13**(2), 165–171 (2000).
17. U. Rubins, "Finger and ear photoplethysmogram waveform analysis by fitting with Gaussians," *Med. Biol. Eng. Comput.* **46**, 1271–1276 (2008).
18. L. Wang et al., "Multi-Gaussian fitting for pulse waveform using weighted least squares and multi-criteria decision making method," *Comput. Biol. Med.* **43**(11), 1661–1672 (2013).
19. J. P. Murgo, "Systolic ejection murmurs in the era of modern cardiology: what do we really know?," *J. Am. Coll. Cardiol.* **32**(6), 1596–602 (1998).
20. R. Couceiro et al., "Multi-Gaussian fitting for the assessment of left ventricular ejection time from the photoplethysmogram," *Proc. IEEE Eng. Med. Biol. Soc.* **2012**, 3951–3954 (2012).
21. K. Lu et al., "A human cardiopulmonary system model applied to the analysis of the Valsalva maneuver," *Am. J. Physiol. Heart Circ. Physiol.* **281**(6), H2661–H2679 (2001).
22. L. Xu et al., "Multi-Gaussian fitting for digital volume pulse using weighted least squares method," in *Proc. IEEE on Information and Automation (ICIA) 2011*, Shenzhen, pp. 544–549, IEEE (2011).
23. A. Grabovskis et al., "Photoplethysmography system for blood pulsation detection in unloaded artery conditions," *Proc. SPIE* **8427**, 84270L (2012).
24. U. Rubins, Z. Marcinkevics, and A. Turkina, "The automated assessment of artery hemodynamic parameters from ultrasound video," in *Proc. Intl. Conf. on Biomedical Engineering*, Chiang Mai, pp. 151–155, IEEE (2012).
25. M. M. Anton et al., "Resistance training increases basal limb blood flow and vascular conductance in aging humans," *J. Appl. Physiol.* **101**(5), 1351–1355 (2006).
26. T. Kawasaki et al., "Noninvasive assessment of the age related changes in stiffness of major branches of the human arteries," *Cardiovasc. Res.* **21**(9), 678–687 (1987).
27. N. Cressie, "Fitting variogram models by weighted least squares," *Math. Geol.* **17**(5), 563–585 (1985).
28. A. Grabovskis et al., "Effect of probe contact pressure on the photoplethysmographic assessment of conduit artery stiffness," *J. Biomed. Opt.* **18**(2), 027004 (2013).
29. J. Calabia et al., "Doppler ultrasound in the measurement of pulse wave velocity: agreement with the Complior method," *Cardiovasc. Ultrasound* **9**(13) (2011).
30. A. Grabovskis et al., "Reliability of hemodynamic parameters measured by a novel photoplethysmography device," in *Int. Federation for Medical and Biological Engineering (IFMBE) Proc.*, Vol. 34, pp. 199–202, Springer Berlin Heidelberg (2011).
31. J. Liu et al., "Effects of cold pressor-induced sympathetic stimulation on the mechanical properties of common carotid and femoral arteries in healthy males," *Heart Vessels* **26**, 214–221 (2011).

Andris Grabovskis received his MSc degree in medical physics from the University of Latvia, Riga, in 2010. Currently, he is the researcher in the Department of Biophotonics at the Institute of Atomic Physics and Spectroscopy, University of Latvia. His research interests include physiological and clinical measurements using contact-probe arterial photoplethysmography, its procedure standardization, and extension of applications toward clinical use and fundamental research.

Zbignevs Marcinkevics received his PhD degree in cardiovascular physiology from the University of Latvia, Riga, in 2013. Currently, he is an adjunct professor of human and animal physiology and the leading researcher at the Institute of Atomic Physics and Spectroscopy at the University of Latvia. His research interests include cardiovascular physiology and development of applications of medical instrumentation in facilitating the diagnostics and treatment of cardiovascular diseases.

Uldis Rubins received his PhD degree in medical physics from the University of Latvia, Riga, in 2009. Currently, he is the leading researcher in the Department of Biophotonics at the Institute of Atomic Physics and Spectroscopy, University of Latvia. His research interests include remote and contact-probe photoplethysmography and hemodynamic pulse waveform analysis. He has authored and co-authored over 20 publications, including peer-reviewed journals and conference proceedings.

Juris Imants Aivars received his medical doctor qualification from Medical Institute, Riga, Latvia, in 1964 and his PhD degree in human and animal physiology from the State University of Leningrad, Russia, in 1986. Currently, he is a professor of human and animal physiology at the University of Latvia, Riga. His research interests include cardiovascular physiology – neurohormonal, myogenic, and endothelium-dependent regulatory mechanisms of arterial vessels, and microcirculation.